

Article

Full-Range Static Method of Calibration for Laser Tracker

Chang'an Hu ^{1,2} , Fei Lv ³, Liang Xue ^{1,*}, Jiangang Li ¹, Xiaoyin Zhong ⁴ and Yue Xu ⁵

¹ National Institute of Measurement and Testing Technology, Chengdu 610021, China; jixiedcd@nimtt.com (C.H.); lijiangang@nimtt.com (J.L.)

² Institute of Fundamental and Frontier Sciences, University of Electronic Science and Technology of China, Chengdu 610054, China

³ School of Computer Science, Chengdu Normal University, Chengdu 611130, China; 153074@cdnu.edu.cn

⁴ Institute of Optics, National Institute of Measurement and Testing Technology, Chengdu 610021, China; zhongxiaoyin@nimtt.com

⁵ School of Automation, Northwestern Polytechnical University, Xi'an 710129, China; xuyue_0325@mail.nwpu.edu.cn

* Correspondence: xueliang@nimtt.com

Abstract: This paper focuses on the challenge of the inability to accurately calibrate the static measurement of a laser tracker across the full scale. To address this issue, this paper proposes to add a hollow corner cube prism on a 50 m high-precision composite guide rail to achieve a double-range measurement of the laser tracker. Data analysis indicated that, in the 77 m identical-directional double-range measurement experiment, the maximum indication error of a single-beam laser interferometer was $-29.5 \mu\text{m}$, and that of a triple-beam laser interferometer was $14.6 \mu\text{m}$, and the measurement indication error was obviously small when the Abbe error was eliminated. The single-point repeatability of the tracker was $0.9 \mu\text{m}$. In the 50 m identical-directional verification experiment, the results of the direct measurement outperformed those of the double-range measurement, and the indication errors under standard conditions were $-4.0 \mu\text{m}$ and $-8.9 \mu\text{m}$, respectively. Overall, the method used in the experiment satisfies the requirements of the laser tracker. In terms of the identical-directional measurement, the measurement uncertainty of the tracker indication error is $U \approx 1.0 \mu\text{m} + 0.2L$ ($k = 2$) $L = (0 \sim 77 \text{ m})$. The proposed method also provides insights for length measurements using other high-precision measuring instruments.



Citation: Hu, C.; Lv, F.; Xue, L.; Li, J.; Zhong, X.; Xu, Y. Full-Range Static Method of Calibration for Laser Tracker. *Electronics* **2023**, *12*, 4709.

<https://doi.org/10.3390/electronics12224709>

Academic Editor: Nakkeeran Kaliyaperumal

Received: 23 October 2023

Revised: 16 November 2023

Accepted: 17 November 2023

Published: 20 November 2023



Copyright: © 2023 by the authors. Licensee MDPI, Basel, Switzerland. This article is an open access article distributed under the terms and conditions of the Creative Commons Attribution (CC BY) license (<https://creativecommons.org/licenses/by/4.0/>).

Keywords: laser tracker; static error; double-range measurement; repeatability experiment; identical-directional measurement; transverse measurement; indication error; measurement uncertainty

1. Introduction

The fast progress in aircraft manufacturing and assembly, heavy-duty systems, antenna measurement, large-scale ion accelerators, and automotive production line measurements, coupled with the increasing complexity of products, has resulted in an ever-growing need for large-scale measurements, thereby making the application of large-scale measuring systems more extensive. The main types of large-scale measuring systems currently in use are laser tracker systems, articulated arm coordinate-measuring machines, laser radar systems, and laser interferometer systems. The calibration of these large-scale measuring systems is of primary significance in ensuring their reliable use, and laboratory calibration serves as the foundation for ensuring the accuracy of large-scale measurement data [1].

Laser tracker systems are extensively utilized in a wide range of applications, including, but not limited to, large-scale coordinate measurement, dynamic measurement, network measurement, attitude measurement, collaborative measurement, and scanning measurement. In terms of accuracy, range, frequency, and application versatility, laser tracker systems offer superior capabilities compared to other large-scale measuring systems. The leading manufacturers of laser tracker systems, including API, FARO, and Leica, provide detailed specifications for both static and dynamic measurement accuracy in their

products. To achieve static measurement accuracy, a high-precision, large-scale guide rail is commonly used. Dynamic measurement accuracy, by contrast, is typically achieved using a circular trajectory generator. Extensive research has been conducted by scholars both domestically and internationally on the measurement accuracy of laser trackers and large-scale calibration methods. Duan et al. evaluated the angular measurement accuracy of laser trackers using the method of direction observation in rounds and the constant-angle method [2]. Ma et al. developed a high-precision, large-scale length calibration system and calibrated laser trackers within a 35 m range [3]. Miao et al. designed and developed an 80 m laser interferometric measurement standard device for the comparative measurement of large-scale measuring instruments [4]. Wang et al. developed a standard circular trajectory generator and proposed parameters and methods for evaluating the dynamic characteristics of laser trackers to assess tracking capability [5]. Pan et al. performed statistical analysis to analyze the dynamic performance of laser trackers by using the deviation from circularity tolerance as the root mean square error [6]. Lv et al. conducted comprehensive research on the dynamic performance of laser trackers. They used a circular trajectory generator to perform the analysis under three different conditions, including equal-spacing measurement at varying distances, equifrequent sampling at varying distances, and measurement with different rotational speeds of a circular trajectory generator at the same distance [7]. Edward et al. explored the performance of laser trackers using an instrument panel and a precision spindle, where the instrument panel enabled planar motion while the precision spindle imitated the circular trajectory generator for circular motion [8]. Additionally, Ma et al. assessed the position and attitude measurement accuracy of laser trackers at varying motion speeds and sampling frequencies using a space circular trajectory generator and indium steel tetrahedron [9]. Xu et al. evaluated the accuracy of trackers using methods such as direction observation, repeated comparative measurement, and free station setting [10]. Liu et al. researched the laser tracker system, focusing on errors related to the movement of the base point, errors in the target tracking system for the rotating mirror, and errors in the perpendicularity between the rotating mirror and the laser beam [11]. Zhu et al. proposed an optimization method for the layout of laser trackers in station measurement based on Monte Carlo simulations. This method aims to enhance the rationality of the station's layout [12]. Zhao et al. integrated the laser tracker with a photogrammetric system to significantly improve tracking accuracy by establishing geometric constraints on common points and employing the graphic rectification method [13]. Acero et al. introduced a platform that utilized capacitive sensors to validate laser trackers [14]. Feng et al. proposed a scheme for laser trackers based on Abbe's principle to improve calibration accuracy in the short range [15]. Conte et al. examined various calibration methods for laser trackers in network measurements [16]. Mitchell et al. demonstrated the use of sensor fusion and registration algorithms in laser tracker systems [17]. Cai et al. constructed a 100 m indoor baseline field using a plane reflector on a 50 m guide rail and analyzed the errors of handheld laser rangefinders [18]. Yang et al. conducted a theoretical study on the feasibility of using optical fibers instead of outdoor baseline fields. They analyzed the impact of various factors, such as coupling, optical waves, and temperature, on the transmission of optical waves in fibers [19]. Shi et al. analyzed the measurement data of laser rangefinders by substituting outdoor baselines with fiber baselines of 30 m, 100 m, and 200 m [20]. Furthermore, China's State Administration for Market Regulation has established specifications for the acceptance testing of laser trackers and specifications for periodic rechecking testing for users to periodically validate the performance of laser trackers [21]. The static measurement accuracy of a laser tracker serves as the basis for exploring its dynamic measurement accuracy. However, no measurement device is described in the literature that calibrates the static measurement accuracy of laser trackers across the entire range. The laser tracker is mainly used for large-scale precision measurement, and its measurement data in the full range must be accurate and reliable. If full-range measurement is impossible, the measurement data may pose a safety hazard. To address this limitation, this study conducts extended research on a large-scale precision guide

rail. The high-precision hollow pyramid prism is adjusted and placed on the movable sliding platform as a reflector to double the optical path of the laser tracker, thus achieving double-range measurement of the laser tracker. The results of this study can not only solve the problem of calibrating the static measurement accuracy of laser trackers across the full scale but also provide insights and methods for static calibration of other large-scale measuring instruments.

2. Laser Tracker

The laser tracker is a portable three-dimensional (3D) coordinate measuring system that operates based on spherical coordinates for measurement. It is equipped with a laser ranging system, laser angular measuring system, control system, dynamic measurement system, laser receiver (including a corner cube retroreflector, measurement head for scanning, scanning probe, and tracking detector), computer with measurement software, base part, and other accessory parts. The laser tracker can realize network measurement. This can be accomplished by employing either a single laser tracker for multiple stations or multiple laser trackers to measure common points, thus enabling the integration of data from laser trackers operating in various coordinate systems or from different laser trackers. Currently, research on laser tracking focuses mainly on the measurement accuracy of laser trackers and the improvement of measurement accuracy after network alignment. The primary factor causing measurement errors in laser tracking systems is range errors. Additionally, factors like laser receivers, measurement environment, and station accuracy also influence measurement accuracy.

The laser tracker relies on the principle of laser interference to measure distances. This principle ensures that the measurement accuracy is equivalent to that of a laser interferometer. Laser trackers are commonly used to measure machine tools, machining centers, and guide rails. Furthermore, laser trackers incorporate a grating disk, offering the advantages of a long measurement distance (80 m) and high measurement accuracy ($\pm(15 \mu\text{m} + 6 \mu\text{m}/\text{m})$). The laser tracker's grating disk utilizes a measurement system based on the principle of multiple-slit diffraction. The grating, an optical component, is created by engraving multiple evenly spaced lines on a glass or metal medium. The accuracy of the grating disk's measurements is determined by the subdivision technique of the Moiré fringe and the photolithography technique used for the grating. Furthermore, the laser tracker system adopts a position-sensitive detector to achieve fast and dynamic measurements. With different laser receivers, the system can perform both contact measurement and non-contact scanning. The system also features a built-in weather station that can adjust in real time according to the ambient temperature, humidity, and air pressure, ensuring accurate measurements. Additionally, temperature sensors can be attached to the object being measured to monitor and adjust for temperature changes in larger targets. When combined with appropriate measurement software that takes into account changes in material properties, more precise measurements can be obtained. These distinct advantages position the system as an outstanding choice for industrial inspection, complex assembly, and the layout of a precise 3D engineering control network.

3. Experimental Scenario and Scheme

3.1. High-Precision Composite Guide Rail and Laser Interferometer System

This device utilizes a high-precision open-type grating as a coarse scale, combined with a laser interferometer system as a fine scale. The motion component consists of a granite base and linear guide rail, with a linear motor as the driving component. This device is capable of performing static measurements and low-speed dynamic measurements within a specific range. The guide rail is made of granite, which possesses outstanding qualities such as a low coefficient of linear expansion, excellent rigidity, high hardness, and non-magnetization. The guide surface is in pristine condition, with no scratches, cracks, delamination, or rust. The guide rail system spans a total length of 57 m, with an effective travel distance of up to 52 m. To ensure high-precision positioning and measurement, the

entire system is equipped with a sliding platform. The linear motion guide rail is used to provide guidance for linear motion, and a grating ruler is mounted on one side of the guide rail for closed-loop control. Motor limit switches and collision protection devices are installed on both ends of the guide rail to ensure safety in case of emergencies.

The laser interferometer system is crucial in the high-precision composite guide rail. It mainly comprises a laser interferometer, an interference mirror, and a reflector. During measurement, one corner cube retroreflector is securely fixed on the beam splitter to form a reference beam of a constant length. The other corner cube retroreflector moves in relation to the beam splitter to form a measurement beam of varying lengths. The laser beam emitted by the laser interferometer is split into two beams—the reflected beam and the transmitted beam—when it reaches the polarization beam splitter. These two beams are then directed toward their respective corner cube retroreflectors and reflected back to the beam splitter. This creates an interference beam in the detector embedded in the laser head. The measurement system consists of three interferometers that also follow the same principle. This system moves linearly on the dual guide rails using grating positioning. These laser interferometers are arranged in an isosceles triangle and labeled as A, B, and C, respectively, as shown in Figure 1. Assuming that the direction of linear motion is along the x -axis when located at a specific position, the readings of the three laser interferometers are x_A , x_B , and x_C , respectively. When the measured target is placed within the isosceles triangle formed by the three laser interferometers, the combination value of the three laser interferometers, denoted as x , can be calculated using the formula: $x = k_1x_A + k_2x_B + k_3x_C$. This allows for the combination value of the three laser interferometers to eliminate the Abbe error for the measured instrument theoretically.



Figure 1. Laser interferometer system (standard value data acquisition).

3.2. Hollow Corner Cube Prism

The hollow corner cube prism, referred to as the hollow retroreflector, plays a crucial role in measuring the optical path length. Similar to a solid corner cube prism, a hollow corner cube prism has the unique ability to return an incoming beam of light directly by 180° . However, hollow corner cube prisms offer an advantage over their solid counterparts. When laser beams hit the surfaces of hollow corner cube prisms, they undergo external reflection. This eliminates wavelength dispersion and path-length variations when beams enter the glass from the air in solid corner cube prisms. As a result, hollow corner cube prisms offer distinct advantages.

This paper discusses the implementation of a hollow corner cube prism that effectively combines three reflectors arranged at a precise 90° angle. This unique structure allows for a remarkable angular accuracy of $0.2''$, ensuring a precise 180° reversal of the optical path. Additionally, it exhibits high wavefront distortion without introducing any other effects on the incident beam. Figure 2 visually depicts the optical path of the hollow corner cube prism, with the incident and exit beams being parallel. The green line represents

the beam of light, and the direction of the arrow represents the direction of the light. It is mounted elastically to maintain stability and minimize stress effects. Custom connections can be established using threaded holes on the backplate of the prism, which offers great convenience. There are two important parameters for the hollow corner cube prism. The first is its angular accuracy, which ensures the generation of highly precise parallel light and reduces the Abbe error. The second is its reflectance, which ensures that the laser can be received by the receiver and provides accurate measurement data.

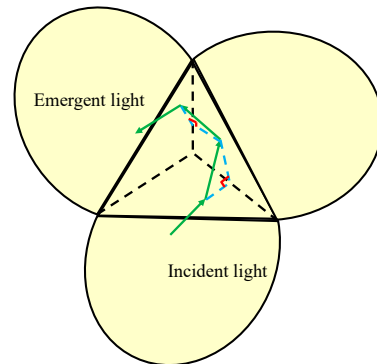


Figure 2. Optical path of the hollow corner cube prism (optical path reflection effect).

The measurement system for the hollow corner cube prism, as depicted in Figure 3, includes a photoelectric autocollimator, a precise angle dividing table, and a display. After preheating, the photoelectric autocollimator is placed parallel to the hollow corner cube prism. The pitch, swing, and tilt angles of the optical axis are measured using the photoelectric autocollimator, precise angle dividing table, and hollow corner cube prism, respectively. Through multiple measurements, the incident angle of the hollow corner cube prism was determined to be $\pm 30^\circ$. The angle error was calculated by taking the maximum value obtained from all the results, which was found to be $0.2''$ within the range of $\pm 10^\circ$.



Figure 3. Angle measuring system based on the hollow corner cube prism. (1—photoelectric autocollimator, 2—display, 3—hollow corner cube prism, 4—precise angle dividing table).

The measurement system for the reflectance of the hollow corner cube prism is shown in Figure 4. The red arrow indicates the laser direction in Figure 4. This system mainly consists of a laser transmitter, a power aperture, a power meter receiver, and a digital display. Similar to the angle measuring system of the hollow corner cube prism, the hollow corner cube prism is aligned parallel to the laser. The power readings before and after placing the hollow corner cube prism were measured separately. After measuring, the power of the incident light was 1.99 mW, and the power of the exit light from the hollow corner cube prism was 1.58 mW. Since the exit light underwent three reflections, the single reflectance of the hollow corner cube prism was 0.92.

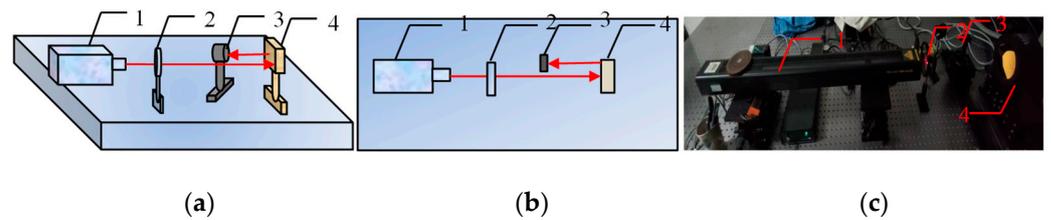


Figure 4. Reflectance measuring system based on the hollow corner cube prism: ((a)—side view, (b)—top view, (c)—physical photo) (1—laser transmitter, 2—power aperture, 3—power meter receiver, 4—hollow corner cube prism).

3.3. Double-Range Measurement System

In the large laboratory, a single-range measurement system is employed, as depicted in Figure 5. However, in Figure 6, an identical-directional double-range measurement system is illustrated, and in Figure 7, a double-range transverse measurement system is shown. Laser interferometers necessitate the use of both an interference mirror and a reflector, whereas laser trackers only require a reflector. The difference between Figure 5 and the other two figures lies in the inclusion of a corner cube prism in the latter. By incorporating the corner cube prism, the reflector of the laser interferometer can be combined with the corner cube prism to achieve double-range measurement. This enables the measurement of large-scale instruments within a shorter distance indoors. In Figures 5–7, the different colored lines representing the laser beams emitted by different laser interferometers and laser trackers. They have no specific meaning. But we can clearly see the changes from the light.

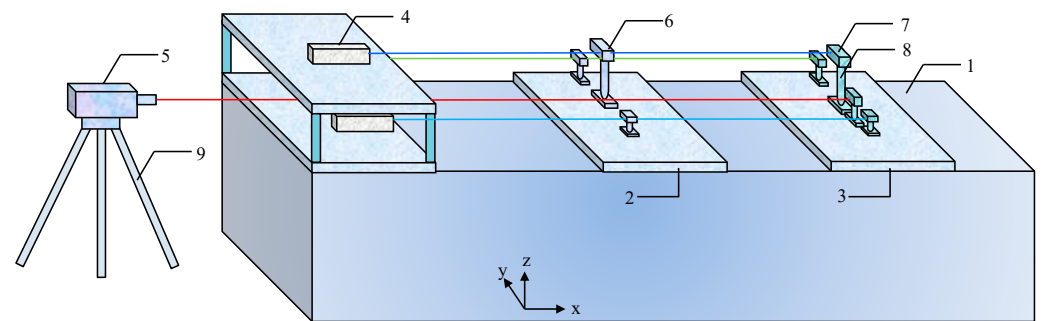


Figure 5. Single-range measurement system (no extended range). (1—guide rail, 2—first sliding platform, 3—second sliding platform, 4—standard laser interferometer, 5—tested laser tracker, 6—interference mirrors, 7—reflectors, 8—fixed mount, 9—tripod with a fine adjustment mechanism).

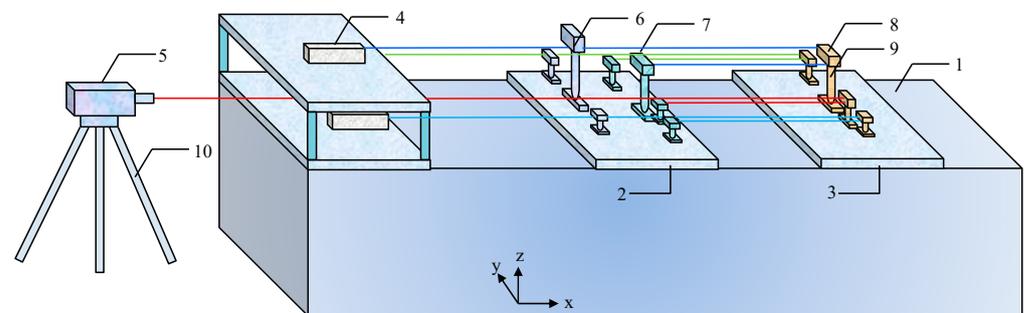


Figure 6. Identical-directional double-range measurement system. (1—guide rail, 2—first sliding platform, 3—second sliding platform, 4—standard laser interferometer, 5—tested laser tracker, 6—interference mirrors, 7—reflectors, 8—corner cube prism, 9—fixed mount, 10—tripod with a fine adjustment mechanism).

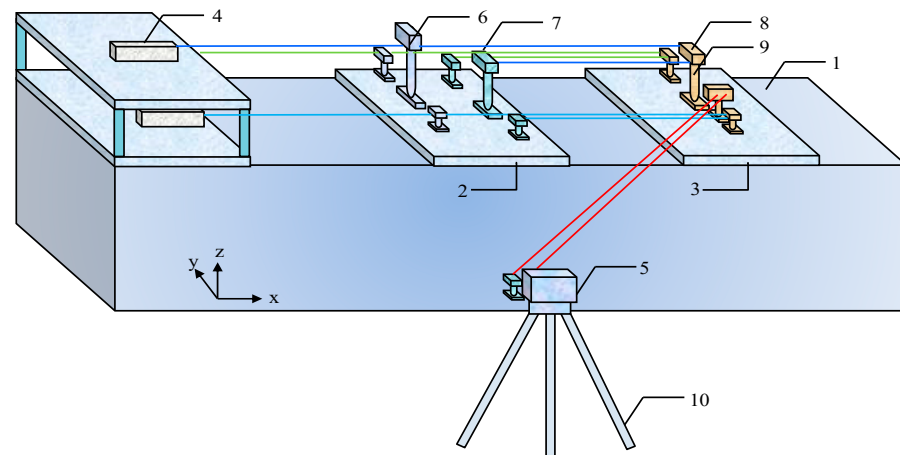


Figure 7. Double-range transverse measurement system. (1—guide rail, 2—first sliding platform, 3—second sliding platform, 4—standard laser interferometer, 5—tested laser tracker, 6—interference mirrors, 7—reflectors, 8—corner cube prism, 9—fixed mount, 10—tripod with a fine adjustment mechanism).

By configuring three laser interferometers in an isosceles triangle and positioning the tested laser interferometer within the spatial range defined by the three laser interferometers, the laser beam of the tested laser interferometer is aligned parallel to those of the three laser interferometers. This configuration eliminates the Abbe error in the system and enhances measurement accuracy. Furthermore, the inclusion of a PTF environmental measurement and compensating system allows for the measurement and compensation of environmental factors, such as temperature, pressure, and humidity, in real time. This enables the correction of measurement data from the laser interferometers, thereby further improving the accuracy of the system's measurements.

3.4. Measurement Procedure

Figures 5–7 all illustrate a double-range measurement system. The process for calibrating this measurement system is identical and can be broken down into the following steps:

In the first step, the standard laser interferometer 4 and the tested laser tracker 5 were activated. The mirrors and the corner cube prism 8 in the dual-range measurement system were adjusted to align the light from the laser interferometer and the laser tracker. This ensured that the optical center of the standard laser interferometer 4 matched that of the corresponding interference mirror 6. Similarly, the optical center of the laser tracker 5 was aligned with that of the reflector 7. The reflector 7 and the corner cube prism 8 were adjusted to receive and reflect the laser emitted by the laser interferometer and the laser tracker.

The laser head of the standard laser interferometer 4 emitted laser beams, spatially parallel to each other, forming a triangular prism. The laser beams were directed towards the corresponding corner cube prism 8 through the corresponding interference mirror 6 and then reflected into the corresponding reflector 7 through the corner cube prism 8. Once reflected by the reflector 7, the laser beams returned to the corner cube prism 8 and underwent reflection again before returning to the interference mirror 6. Interference occurred within the interference mirror 6, and the interference light entered the detector of the standard laser interferometer 4. The laser beams were reflected by the reflector 7 and the corner cube prism 8, effectively doubling the optical path.

The laser beams generated by the laser head of the tested laser tracker 5 were contained within a prism-shaped enclosure, with the laser path running parallel to that of the standard laser interferometer 4. The laser beams emitted by the tested laser tracker 5 were then reflected by the corner cube prism 8 and directed towards the reflector 7. The laser beams

underwent reflection by the reflector 7 and the corner cube prism 8, doubling the optical path.

In the second step, the dehumidification system and the air-conditioning system were activated to regulate the humidity and temperature levels of the indoor air within a predetermined range.

In the third step, the appropriate sampling frequency and sampling interval were determined to collect the displacement data from both the standard laser interferometer 4 and the tested laser tracker 4. Throughout the collection process, the first sliding platform 2 remained stationary, while the automatic control system managed the movement of the second sliding platform 3 along the x-axis. Data were collected systematically at regular intervals until all displacement data were acquired. In the PTF environment, multiple sensors measured different parameters: The first temperature sensor targeted the indoor temperature, the second temperature sensor measured the temperature of the tested target, the pressure sensor was responsible for the air pressure, and the humidity sensor was used to measure the air humidity. These sensors collected data and continuously adjusted the values of the laser interferometer in the PTF environment using the Edlen formula, resulting in accurate measurement values of the laser interferometer at each position.

In the fourth step, the collected displacement data were assessed by comparing the nominal values (the measured values at each position from the standard laser interferometer 4) with the displacement values at each position from the tested laser tracker 5. This comparison helped to identify the measurement error of the tested laser tracker 5 and determine if it fell within the acceptable range. By doing so, this study determined if the tested laser tracker met the required standards.

3.5. Experimental Scheme

The primary instruments employed in the experiment included a laser interferometer, a hollow corner cube prism, and a laser tracker. The experiment was mainly divided into five parts for data analysis, including an identical-directional 77 m double-range measurement experiment conducted in a controlled environment setting, an identical-directional single-point repeatability experiment conducted in a controlled environment setting, an identical-directional 50 m verification experiment conducted in both a controlled environment setting and a laboratory setting, a transverse measurement experiment conducted in a controlled environment setting, and an evaluation of measurement uncertainty for the indication error. The study utilized a Leica Absolute Tracker AT930 with instrument number 750,397. Additionally, a Keysight 5519 B laser interferometer was applied. The controlled environment setting for the experiment was a temperature of 20 °C, humidity of 50% RH, and air pressure of 101.3 kPa, while the laboratory setting had a temperature of 19 °C, humidity of 52% RH, and air pressure of 94.48 kPa.

4. Experiment

4.1. Identical-Directional 77-Meter Double-Range Measurement Experiment

The double-range measurement experiment using a laser tracker was conducted twice. Table 1 displays the results of the first triple-beam measurement, which involved measuring a range of 77 m in a controlled environment setting. The table reveals that the laser tracker exhibited a maximum indication error of 14.6 µm at the 37 m position. Table 2 presents the results of the second measurement, where the maximum indication error of the laser tracker was 13.9 µm at the 76 m position. All the results from both measurements satisfy the requirement for indication errors of $\pm(15 \mu\text{m} + 6 \mu\text{m}/\text{m})$. The experimentation confirms that the double-range measurement method satisfactorily fulfills the criteria for identical-directional measurement of the laser tracker. The maximum indication error of the two measurements was 14.6 µm. The coordinates of the base point during the first measurement were -927.0599 mm , 2655.6821 mm , and 7.0187 mm , and the distance from the base point to the zero position of the tracker was approximately 3 m. The laser tracker used in this

experiment had a measurement range of 0 to 80 m, allowing for a maximum range of 77 m for the double-range measurement.

Table 1. Results from the first 77-m double-range measurement experiment using a triple-beam laser interferometer in a controlled environment setting (identical-directional).

Triple-Beam Interferometer Fitted Value (mm)	Interferometer Nominal Value (mm)	Tracker Measured Value (mm)	Indication Error (μm)	Triple-Beam Interferometer Fitted Value (mm)	Interferometer Nominal Value (mm)	Tracker Measured Value (mm)	Indication Error (μm)
499.9910	999.9820	999.9822	0.2	19,999.8217	39,999.6434	39,999.6460	2.6
999.9767	1999.9534	1999.9535	0.1	20,499.8225	40,999.6450	40,999.6504	5.4
1499.9696	2999.9392	2999.9382	-1.0	20,999.8330	41,999.6660	41,999.6686	2.6
1999.9586	3999.9172	3999.9168	-0.4	21,499.8330	42,999.6660	42,999.6713	5.3
2499.9778	4999.9556	4999.9480	-7.6	21,999.8404	43,999.6808	43,999.6840	3.2
2999.9671	5999.9342	5999.9261	-8.1	22,499.8636	44,999.7272	44,999.7271	-0.1
3499.9620	6999.9240	6999.9164	-7.6	22,999.8728	45,999.7456	45,999.7438	-1.8
3999.9482	7999.8964	7999.8909	-5.5	23,499.8721	46,999.7442	46,999.7444	0.2
4499.9323	8999.8646	8999.8600	-4.6	23,999.8749	47,999.7498	47,999.7515	1.7
4999.9152	9999.8304	9999.8277	-2.7	24,499.8885	48,999.7770	48,999.7772	0.2
5499.9067	10,999.8134	10,999.8110	-2.4	24,999.8846	49,999.7692	49,999.7693	0.1
5999.8947	11,999.7894	11,999.7895	0.1	25,499.8929	50,999.7858	50,999.7861	0.3
6499.8749	12,999.7498	12,999.7509	1.1	25,999.8963	51,999.7926	51,999.7917	-0.9
6999.8830	13,999.7660	13,999.7619	-4.1	26,499.8896	52,999.7792	52,999.7833	4.1
7499.8617	14,999.7234	14,999.7199	-3.5	26,999.8949	53,999.7898	53,999.7918	2.0
7999.8587	15,999.7174	15,999.7135	-3.9	27,499.9051	54,999.8102	54,999.8145	4.3
8499.8486	16,999.6972	16,999.6932	-4.0	27,999.9044	55,999.8088	55,999.8135	4.7
8999.8544	17,999.7088	17,999.7034	-5.4	28,499.9153	56,999.8306	56,999.8359	5.3
9499.8370	18,999.6740	18,999.6720	-2.0	28,999.9337	57,999.8674	57,999.8731	5.7
9999.8404	19,999.6808	19,999.6775	-3.3	29,499.9173	58,999.8346	58,999.8381	3.5
10,499.8382	20,999.6764	20,999.6693	-7.1	29,999.9255	59,999.8510	59,999.8563	5.3
10,999.8309	21,999.6618	21,999.6594	-2.4	30,499.9579	60,999.9158	60,999.9100	-5.8
11,499.8165	22,999.6330	22,999.6307	-2.3	30,999.9648	61,999.9296	61,999.9260	-3.6
11,999.8096	23,999.6192	23,999.6181	-1.1	31,499.9516	62,999.9032	62,999.9037	0.5
12,499.7944	24,999.5888	24,999.5890	0.2	31,999.9579	63,999.9158	63,999.9153	-0.5
12,999.7977	25,999.5954	25,999.5968	1.4	32,499.9487	64,999.8974	64,999.8984	1.0
13,499.8125	26,999.6250	26,999.6257	0.7	32,999.9576	65,999.9152	65,999.9149	-0.3
13,999.7969	27,999.5938	27,999.5941	0.3	33,499.9554	66,999.9108	66,999.9164	5.6
14,499.8052	28,999.6104	28,999.6073	-3.1	33,999.9554	67,999.9108	67,999.9118	1.0
14,999.7981	29,999.5962	29,999.5945	-1.7	34,499.9397	68,999.8794	68,999.8816	2.2
15,499.7997	30,999.5994	30,999.5977	-1.7	34,999.9347	69,999.8694	69,999.8781	8.7
15,999.8011	31,999.6022	31,999.6006	-1.6	35,499.9425	70,999.8850	70,999.8931	8.1
16,499.7999	32,999.5998	32,999.5986	-1.2	35,999.9308	71,999.8616	71,999.8702	8.6
16,999.7988	33,999.5976	33,999.5984	0.8	36,499.9286	72,999.8572	72,999.8686	11.4
17,499.8008	34,999.6016	34,999.6031	1.5	36,999.9129	73,999.8258	73,999.8404	14.6
17,999.8153	35,999.6306	35,999.6325	1.9	37,499.9160	74,999.8320	74,999.8411	9.1
18,499.8061	36,999.6122	36,999.6146	2.4	37,999.8982	75,999.7964	75,999.8106	14.2
18,999.8062	37,999.6124	37,999.6183	5.9	38,499.9266	76,999.8532	76,999.8614	8.2
19,499.8089	38,999.6178	38,999.6217	3.9	/	/	/	/

Tables 3 and 4 present the indication errors observed under the condition of a single-beam laser interferometer. The laser interferometer C in close proximity to the laser tracker provided the measured values used in Tables 3 and 4. The recorded positions were approximations. According to Table 3, it can be observed that the maximum indication error was 29.4 μm at a measurement position of 76 m. According to the data presented in Table 4, it is evident that the position at 61 m exhibited a maximum indication error of -29.5 μm . The maximum indication error was slightly greater under the single-beam condition than the triple-beam condition. Both measurement results obtained under the single-beam condition satisfy the measurement requirements for the indication error of the laser tracker.

Table 2. Results from the second 77-m double-range measurement experiment using a triple-beam laser interferometer in a controlled environment setting (identical-directional).

Interferometer Nominal Value (mm)	Tracker Measured Value (mm)	Indication Error (μm)	Interferometer Nominal Value (mm)	Tracker Measured Value (mm)	Indication Error (μm)
999.9828	999.9831	0.3	39,999.6418	39,999.6438	2.0
1999.9550	1999.9560	1.0	40,999.6434	40,999.6484	5.0
2999.9424	2999.9418	−0.6	41,999.6622	41,999.6654	3.2
3999.9190	3999.9194	0.4	42,999.6652	42,999.6691	3.9
4999.9588	4999.9494	−9.4	43,999.6792	43,999.6812	2.0
5999.9334	5999.9266	−6.8	44,999.7254	44,999.7256	0.2
6999.9252	6999.9181	−7.1	45,999.7416	45,999.7402	−1.4
7999.8980	7999.8918	−6.2	46,999.7416	46,999.7404	−1.2
8999.8646	8999.8615	−3.1	47,999.7502	47,999.7478	−2.4
9999.8314	9999.8294	−2.0	48,999.7732	48,999.7739	0.7
10,999.8178	10,999.8136	−4.2	49,999.7654	49,999.7665	1.1
11,999.7918	11,999.7920	0.2	50,999.7832	50,999.7831	−0.1
12,999.7516	12,999.7527	1.1	51,999.7866	51,999.7890	2.4
13,999.7666	13,999.7648	−1.8	52,999.7754	52,999.7790	3.6
14,999.7250	14,999.7209	−4.1	53,999.7874	53,999.7879	0.5
15,999.7200	15,999.7159	−4.1	54,999.8056	54,999.8097	4.1
16,999.6988	16,999.6947	−4.1	55,999.8032	55,999.8088	5.6
17,999.7100	17,999.7054	−4.6	56,999.8312	56,999.8312	0.0
18,999.6750	18,999.6735	−1.5	57,999.8650	57,999.8704	5.4
19,999.6812	19,999.6795	−1.7	58,999.8298	58,999.8334	3.6
20,999.6764	20,999.6697	−6.7	59,999.8454	59,999.8497	4.3
21,999.6618	21,999.6593	−2.5	60,999.9110	60,999.9041	−6.9
22,999.6312	22,999.6300	−1.2	61,999.9242	61,999.9194	−4.8
23,999.6192	23,999.6193	0.1	62,999.9016	62,999.8972	−4.4
24,999.5900	24,999.5903	0.3	63,999.9110	63,999.9084	−2.6
25,999.5974	25,999.5975	0.1	64,999.8932	64,999.8911	−2.1
26,999.6270	26,999.6260	−1.0	65,999.9074	65,999.9073	−0.1
27,999.5934	27,999.5932	−0.2	66,999.9090	66,999.9095	0.5
28,999.6112	28,999.6065	−4.7	67,999.9030	67,999.9070	4.0
29,999.5944	29,999.5928	−1.6	68,999.8716	68,999.8748	3.2
30,999.5982	30,999.5964	−1.8	69,999.8644	69,999.8689	4.5
31,999.6002	31,999.5994	−0.8	70,999.8772	70,999.8855	8.3
32,999.5968	32,999.5970	0.2	71,999.8538	71,999.8617	7.9
33,999.5938	33,999.5962	2.4	72,999.8538	72,999.8598	6.0
34,999.6016	34,999.6019	0.3	73,999.8226	73,999.8301	7.5
35,999.6298	35,999.6307	0.9	74,999.8242	74,999.8327	8.5
36,999.6100	36,999.6141	4.1	75,999.7886	75,999.8025	13.9
37,999.6130	37,999.6174	4.4	76,999.8482	76,999.8504	2.2
38,999.6138	38,999.6183	4.5	/	/	/

The indication errors from Tables 1–4 are visually depicted in Figure 8, where the red dot corresponds to the first measurement result obtained from the triple-beam method, while the blue dot represents the second measurement result from the same method. Additionally, the green cross indicates the first measurement result obtained from the single-beam method, while the pink cross represents the second measurement result from the same method. By analyzing this data, this study draws three conclusions, as follows:

First, the oscillation in the error for the measurement using the triple-beam laser interferometer is smaller compared to the measurement using the single-beam laser interferometer. The results obtained from the two measurements using the triple-beam laser interferometer, which eliminates the Abbe error, are significantly better than those obtained from the two measurements using the single-beam laser interferometer.

Second, when the triple-beam laser was used for measurement, the maximum measurement repeatability was 7.1 μm , which occurred at 71 m. When the single-beam laser

was used for measurement, the maximum measurement repeatability was 11 μm , which occurred at 77 m. The repeatability of the two measurement results was good.

Lastly, the indication errors exhibit both positive and negative values, resulting in a sawtooth pattern. This pattern suggests that the laser tracker's measured values align closely with the nominal values of the interferometer, indicating a high level of measurement accuracy.

Table 3. Indication errors from the first 77-m double-range measurement experiment using a single-beam laser interferometer in a controlled environment setting (identical-directional).

Position (m)	Indication Error (μm)	Position (m)	Indication Error (μm)	Position (m)	Indication Error (μm)	Position (m)	Indication Error (μm)
1	1.0	21	-20.1	41	13.6	61	-27.6
2	3.1	22	-6.6	42	8.4	62	-15.4
3	0.0	23	-4.1	43	11.1	63	-10.3
4	4.2	24	-1.1	44	8.2	64	-10.5
5	-18.4	25	3.0	45	-3.3	65	-4.0
6	-21.7	26	3.0	46	-10.2	66	-6.9
7	-18.6	27	0.7	47	-5.6	67	2.4
8	-14.3	28	0.3	48	-2.5	68	-2.2
9	-10.2	29	-9.9	49	-4.0	69	-1.2
10	-5.3	30	-5.1	50	-4.1	70	18.7
11	-2.4	31	-5.9	51	-2.9	71	18.1
12	2.3	32	-4.8	52	-5.1	72	18.6
13	6.7	33	-3.0	53	9.9	73	24.8
14	-8.7	34	0.8	54	2.8	74	27.8
15	-8.7	35	1.5	55	5.9	75	20.7
16	-9.1	36	3.5	56	8.9	76	29.4
17	-10.0	37	9.2	57	7.7	77	9.8
18	-13.4	38	16.7	58	9.9	/	/
19	-5.8	39	12.3	59	6.1	/	/
20	-10.1	40	9.2	60	8.7	/	/

Table 4. Indication errors from the second 77-m double-range measurement experiment using a single-beam laser interferometer in a controlled environment setting (identical-directional).

Position (m)	Indication Error (μm)	Position (m)	Indication Error (μm)	Position (m)	Indication Error (μm)	Position (m)	Indication Error (μm)
1	1.3	21	-19.7	41	11.6	61	-29.5
2	3.4	22	-6.7	42	9.2	62	-18.2
3	-0.6	23	-2.8	43	8.9	63	-16.8
4	4.6	24	0.1	44	5.4	64	-13.4
5	-21.8	25	2.3	45	-4.8	65	-11.3
6	-19.6	26	1.7	46	-9.8	66	-6.7
7	-19.5	27	-1.0	47	-9.6	67	-4.5
8	-16.4	28	-0.6	48	-10.0	68	0.8
9	-8.7	29	-12.7	49	-3.5	69	-0.2
10	-4.6	30	-4.8	50	-3.1	70	9.5
11	-6.8	31	-5.2	51	-5.9	71	18.3
12	2.0	32	-4.2	52	0.0	72	17.9
13	6.5	33	-0.6	53	9.4	73	16.0
14	-5.8	34	2.4	54	-1.1	74	17.5
15	-9.5	35	0.3	55	5.1	75	20.1
16	-9.7	36	1.7	56	8.0	76	29.1
17	-10.3	37	12.5	57	-0.8	77	-1.2
18	-13.4	38	12.0	58	7.2	/	/
19	-6.1	39	12.9	59	5.2	/	/
20	-8.1	40	7.0	60	5.9	/	/

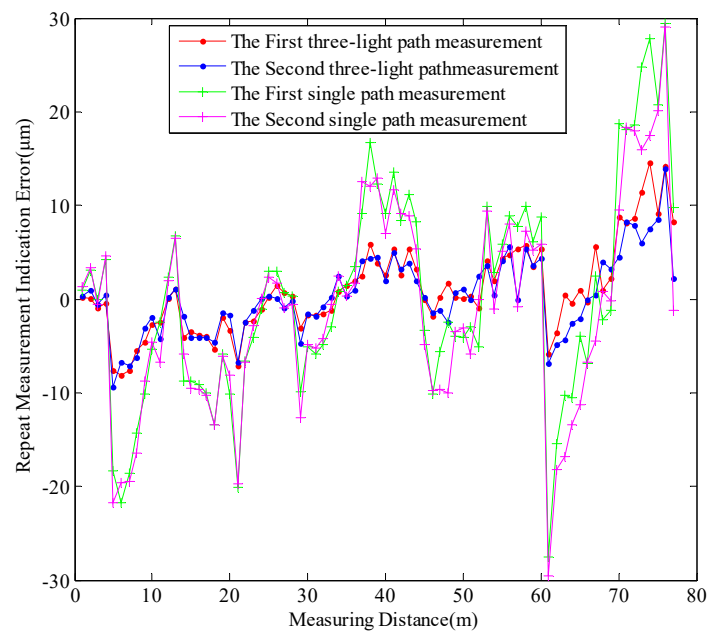


Figure 8. Comparison of indication errors between two double-range measurements.

4.2. Identical-Directional Single-Point Repeatability Experiment

The repeatability experiment was carried out at three points, namely the 65 m, 70 m, and 77 m positions, within a controlled environment setting. The results are shown in Table 5. Upon conducting the measurements twice, the average values at the 65 m position were determined to be 64,999.8976 mm and 64,999.8906 mm, respectively, with a standard deviation of 0.5 µm. At the 70 m position, the average values were 69,999.8781 mm and 69,999.8699 mm, with standard deviations of 0.1 µm and 0.6 µm, respectively. At a distance of 77 m, the average values were 76,999.8588 mm and 76,999.8506 mm, with standard deviations of 0.9 µm and 0.1 µm, respectively. Based on the data analysis, it is evident that the repeatability is excellent across all three positions. The highest standard deviation, observed at the 77 m position, was 0.9 µm.

Table 5. Results of two single-point repeatability experiment measurements at distances of 65 m, 70 m, and 77 m (identical-directional).

Measurement No.	Tracker Measured Value (mm)					
	First Measurement			Second Measurement		
/						
1	64,999.8984	69,999.8781	76,999.8614	64,999.8911	69,999.8689	76,999.8504
2	64,999.8974	69,999.8780	76,999.8587	64,999.8903	69,999.8692	76,999.8507
3	64,999.8972	69,999.8780	76,999.8585	64,999.8908	69,999.8694	76,999.8506
4	64,999.8968	69,999.8781	76,999.8583	64,999.8907	69,999.8695	76,999.8507
5	64,999.8972	69,999.8781	76,999.8584	64,999.8903	69,999.8699	76,999.8507
6	64,999.8978	69,999.8782	76,999.8586	64,999.8898	69,999.8700	76,999.8507
7	64,999.8978	69,999.8781	76,999.8585	64,999.8900	69,999.8700	76,999.8506
8	64,999.8978	69,999.8781	76,999.8588	64,999.8902	69,999.8706	76,999.8504
9	64,999.8978	69,999.8780	76,999.8586	64,999.8911	69,999.8706	76,999.8504
10	64,999.8979	69,999.8780	76,999.8585	64,999.8915	69,999.8708	76,999.8507
Average value (mm)	64,999.8976	69,999.8781	76,999.8588	64,999.8906	69,999.8699	76,999.8506
Standard deviation (µm)	0.5	0.1	0.9	0.5	0.6	0.1

4.3. Identical-Directional 50-Meter Verification Experiment

4.3.1. 50-Meter Direct Measurement

Table 6 presents the measurement data obtained through direct measurement in a controlled environment setting within a 50 m range. The fitted values of the three laser in-

terferometers, namely A, B, and C, were obtained through a fitting process. The coefficients utilized were $k_1 = 3/14$, $k_2 = 3/14$, and $k_3 = 4/7$, with the total sum of coefficients equaling 1. The fitted values of the three laser interferometers corresponded to the nominal values of the laser interferometers. Upon examining the table, it is evident that the indication error reached its maximum value of $-4.0 \mu\text{m}$, with this maximum error occurring at the position located at a distance of 3 m. The requirements for laser tracking indication errors can be fulfilled at all positions.

Table 6. Results from the 50 m direct measurement in a controlled environment setting (identical-directional verification experiment).

Interferometer A (mm)	Interferometer B (mm)	Interferometer C (mm)	Triple-Beam Interferometer Fitted Value/ Interferometer Nominal Value (mm)	Tracker Measured Value (mm)	Indication Error (μm)
999.9803	999.9796	999.9779	999.9788	999.9780	-0.8
1999.9628	1999.9640	1999.9585	1999.9606	1999.9592	-1.4
2999.9561	2999.9600	2999.9741	2999.9672	2999.9632	-4.0
3999.9392	3999.9453	3999.9536	3999.9487	3999.9452	-3.5
4999.9121	4999.9155	4999.9180	4999.9162	4999.9135	-2.7
5999.8940	5999.8989	5999.8955	5999.8959	5999.8944	-1.5
6999.8892	6999.8706	6999.8857	6999.8832	6999.8805	-2.7
7999.8638	7999.8472	7999.8618	7999.8591	7999.8566	-2.5
8999.8584	8999.8398	8999.8584	8999.8544	8999.8509	-3.5
9999.8447	9999.8272	9999.8447	9999.8410	9999.8380	-3.0
10,999.8350	10,999.8193	10,999.8311	10,999.8294	10,999.8268	-2.6
11,999.8174	11,999.7979	11,999.8086	11,999.8082	11,999.8060	-2.2
12,999.8076	12,999.7871	12,999.7969	12,999.7971	12,999.7947	-2.4
13,999.8047	13,999.7842	13,999.7959	13,999.7953	13,999.7926	-2.7
14,999.8047	14,999.7793	14,999.7969	14,999.7948	14,999.7919	-2.9
15,999.8086	15,999.7822	15,999.8008	15,999.7985	15,999.7954	-3.1
16,999.8086	16,999.7813	16,999.7969	16,999.7960	16,999.7933	-2.7
17,999.8242	17,999.7988	17,999.8106	17,999.8110	17,999.8096	-1.4
18,999.8106	18,999.8047	18,999.7969	18,999.8015	18,999.8013	-0.2
19,999.8203	19,999.8184	19,999.8125	19,999.8154	19,999.8154	0.0
20,999.8301	20,999.8281	20,999.8242	20,999.8263	20,999.8257	-0.6
21,999.8359	21,999.8359	21,999.8340	21,999.8348	21,999.8340	-0.8
22,999.8574	22,999.8613	22,999.8691	22,999.8650	22,999.8632	-1.8
23,999.8633	23,999.8633	23,999.8731	23,999.8689	23,999.8661	-2.8
24,999.8711	24,999.8750	24,999.8809	24,999.8775	24,999.8760	-1.5
25,999.8828	25,999.8867	25,999.8906	25,999.8881	25,999.8861	-2.0
26,999.8848	26,999.8848	26,999.8867	26,999.8859	26,999.8843	-1.6
27,999.8945	27,999.8965	27,999.8945	27,999.8949	27,999.8945	-0.4
28,999.9258	28,999.9258	28,999.9258	28,999.9258	28,999.9240	-1.8
29,999.9160	29,999.9160	29,999.9141	29,999.9149	29,999.9151	0.2
30,999.9453	30,999.9434	30,999.9590	30,999.9527	30,999.9504	-2.3
31,999.9434	31,999.9375	31,999.9512	31,999.9466	31,999.9445	-2.1
32,999.9453	32,999.9375	32,999.9453	32,999.9436	32,999.9440	0.4
33,999.9453	33,999.9375	33,999.9453	33,999.9436	33,999.9420	-1.6
34,999.9297	34,999.9219	34,999.9180	34,999.9213	34,999.9220	0.7
35,999.9258	35,999.9180	35,999.9141	35,999.9174	35,999.9185	1.1
36,999.9102	36,999.9063	36,999.8945	36,999.9004	36,999.9031	2.7
37,999.9023	37,999.8906	37,999.8789	37,999.8864	37,999.8883	1.9
38,999.9023	38,999.9023	38,999.8984	38,999.9001	38,999.9003	0.2
39,999.8984	39,999.8945	39,999.8945	39,999.8954	39,999.8953	-0.1
40,999.8750	40,999.8711	40,999.8633	40,999.8675	40,999.8681	0.6
41,999.8672	41,999.8633	41,999.8594	41,999.8619	41,999.8617	-0.2
42,999.8516	42,999.8594	42,999.8594	42,999.8577	42,999.8573	-0.4
43,999.8242	43,999.8359	43,999.8320	43,999.8312	43,999.8310	-0.2
44,999.8008	44,999.8086	44,999.8047	44,999.8047	44,999.8059	1.2
45,999.7813	45,999.7930	45,999.7852	45,999.7860	45,999.7872	1.2
46,999.7344	46,999.7227	46,999.7266	46,999.7274	46,999.7287	1.3
47,999.7109	47,999.6992	47,999.6992	47,999.7017	47,999.7018	0.1
48,999.6719	48,999.6563	48,999.6523	48,999.6574	48,999.6584	1.0
49,999.6367	49,999.6211	49,999.6133	49,999.6200	49,999.6230	3.0

4.3.2. 50-Meter Double-Range Measurement

Table 7 presents the results achieved through the utilization of the double-range measurement within a range of 50 m in a controlled environment setting. The table reveals that the indication error of the laser tracker reached its maximum value of $-8.9 \mu\text{m}$ at the 6 m position. The requirements of laser tracking indication errors can be satisfied at all locations.

Table 7. Results of the 50-meter double-range measurement in a controlled environment setting (identical-directional verification experiment).

Triple-Beam Interferometer Fitted Value (mm)	Interferometer Nominal Value (mm)	Tracker Measured Value (mm)	Indication Error (μm)	Triple-Beam Interferometer Fitted Value (mm)	Interferometer Nominal Value (mm)	Tracker Measured Value (mm)	Indication Error (μm)
499.9922	999.9844	999.9846	0.2	12,999.7972	25,999.5944	25,999.5966	2.2
999.9783	1999.9566	1999.9576	1.0	13,499.8136	26,999.6272	26,999.6264	-0.8
1499.9716	2999.9432	2999.9433	0.1	13,999.7967	27,999.5934	27,999.5929	-0.5
1999.9599	3999.9198	3999.9207	0.9	14,499.8054	28,999.6108	28,999.6060	-4.8
2499.9781	4999.9562	4999.9509	-5.3	14,999.7973	29,999.5946	29,999.5916	-3.0
2999.9685	5999.9370	5999.9281	-8.9	15,499.7974	30,999.5948	30,999.5952	0.4
3499.9632	6999.9264	6999.9185	-7.9	15,999.8006	31,999.6012	31,999.5982	-3.0
3999.9483	7999.8966	7999.8926	-4.0	16,499.7980	32,999.5960	32,999.5964	0.4
4499.9328	8999.8656	8999.8618	-3.8	16,999.7980	33,999.5960	33,999.5953	-0.7
4999.9146	9999.8292	9999.8294	0.2	17,499.8004	34,999.6008	34,999.5998	-1.0
5499.9076	10,999.8152	10,999.8150	-0.2	17,999.8140	35,999.6280	35,999.6282	0.2
5999.8965	11,999.7930	11,999.7923	-0.7	18,499.8030	36,999.6060	36,999.6106	4.6
6499.8757	12,999.7514	12,999.7531	1.7	18,999.8054	37,999.6108	37,999.6143	3.5
6999.8841	13,999.7682	13,999.7638	-4.4	19,499.8072	38,999.6144	38,999.6159	1.5
7499.8613	14,999.7226	14,999.7206	-2.0	19,999.8198	39,999.6396	39,999.6423	2.7
7999.8601	15,999.7202	15,999.7160	-4.2	20,499.8217	40,999.6434	40,999.6460	2.6
8499.8511	16,999.7022	16,999.6951	-7.1	20,999.8291	41,999.6582	41,999.6634	5.2
8999.8550	17,999.7100	17,999.7053	-4.7	21,499.8318	42,999.6636	42,999.6660	2.4
9499.8392	18,999.6784	18,999.6731	-5.3	21,999.8354	43,999.6708	43,999.6789	8.1
9999.8423	19,999.6846	19,999.6794	-5.2	22,499.8601	44,999.7202	44,999.7226	2.4
10,499.8388	20,999.6776	20,999.6702	-7.4	22,999.8689	45,999.7378	45,999.7367	-1.1
10,999.8315	21,999.6630	21,999.6587	-4.3	23,499.8693	46,999.7386	46,999.7364	-2.2
11,499.8146	22,999.6292	22,999.6287	-0.5	23,999.8739	47,999.7478	47,999.7438	-4.0
11,999.8085	23,999.6170	23,999.6189	1.9	24,499.8857	48,999.7714	48,999.7700	-1.4
12,499.7935	24,999.5870	24,999.5889	1.9	24,999.8818	49,999.7636	49,999.7636	0.0

4.3.3. 50-Meter Double-Range Measurement in a Laboratory Setting

Table 8 displays the results acquired through the utilization of the double-range measurement within a range of 50 m in a laboratory setting. The indication error reached its maximum value of $-8.3 \mu\text{m}$ at the 21 m position. The requirements of laser tracking indication errors can be satisfied at all locations.

To analyze the results of the laser tracker within a 50 m range more intuitively, the indication errors of the results in Tables 6–8 are graphically displayed, resulting in Figure 9, which shows a comparison of the indication errors in the 50 m verification experiment. The blue curve depicts the direct measurement result taken within a 50 m range in a controlled environment setting. The red curve represents the double-range measurement result within the 50 m range in a controlled environment setting. Lastly, the green curve illustrates the double-range measurement result within the 50 m range conducted in a laboratory setting. From Figure 9, the following four conclusions can be drawn:

First, the oscillation of the indication error is the smallest in direct measurement and significantly smaller than in the double-range measurement. The oscillation of indication errors is relatively large in the double-range measurement.

Second, the red and blue curves have similar patterns; the repeatability of the measurement results can be obtained by subtracting the indication errors of the two groups, and the maximum difference was $8.5 \mu\text{m}$, which occurred at 44 m. It can be seen that the repeatability is good during double-range measurement.

Third, the curves depicting the indication errors for all three measurements exhibit a sawtooth pattern, which suggests that the results of the laser tracker closely align with those of the laser interferometer. This observation serves as evidence of the laser tracker’s high measurement accuracy.

Lastly, the indication errors of all three measurements meet the requirements of the laser tracking indication errors, indirectly verifying the reliability of the identical-directional double-range measurement for the laser tracker.

Table 8. Results of the 50-meter double-range measurement in a laboratory setting (identical-directional verification experiment).

Triple-Beam Interferometer Fitted Value (mm)	Interferometer Nominal Value (mm)	Tracker Measured Value (mm)	Indication Error (μm)	Triple-Beam Interferometer Fitted Value (mm)	Interferometer Nominal Value (mm)	Tracker Measured Value (mm)	Indication Error (μm)
500.0033	1000.0066	1000.0059	−0.7	13,000.0273	26,000.0546	26,000.0525	−2.1
999.9975	1999.9950	1999.9965	1.5	13,500.0499	27,000.0998	27,000.0992	−0.6
1499.9989	2999.9978	3000.0002	2.4	14,000.0437	28,000.0874	28,000.0836	−3.8
1999.9974	3999.9948	3999.9943	−0.5	14,500.0592	29,000.1184	29,000.1138	−4.6
2500.0242	5000.0484	5000.0415	−6.9	15,000.0596	30,000.1192	30,000.1174	−1.8
3000.0221	6000.0442	6000.0361	−8.1	15,500.0702	31,000.1404	31,000.1379	−2.5
3500.0254	7000.0508	7000.0445	−6.3	16,000.0798	32,000.1596	32,000.1591	−0.5
4000.0214	8000.0428	8000.0362	−6.6	16,500.0871	33,000.1742	33,000.1740	−0.2
4500.0144	9000.0288	9000.0243	−4.5	17,000.0949	34,000.1898	34,000.1908	1.0
5000.0060	10,000.0120	10,000.0093	−2.7	17,500.1066	35,000.2132	35,000.2121	−1.1
5500.0062	11,000.0124	11,000.0112	−1.2	18,000.1293	36,000.2586	36,000.2596	1.0
6000.0041	12,000.0082	12,000.0070	−1.2	18,500.1283	37,000.2566	37,000.2590	2.4
6499.9911	12,999.9822	12,999.9828	0.6	19,000.1385	38,000.2770	38,000.2794	2.4
7000.0081	14,000.0162	14,000.0116	−4.6	19,500.1479	39,000.2958	39,000.2991	3.3
7499.9946	14,999.9892	14,999.9856	−3.6	20,000.1689	40,000.3378	40,000.3410	3.2
8000.0005	16,000.0010	15,999.9974	−3.6	20,500.1807	41,000.3614	41,000.3639	2.5
8500.0007	17,000.0014	16,999.9949	−6.5	21,000.1982	42,000.3964	42,000.3993	2.9
9000.0142	18,000.0284	18,000.0223	−6.1	21,500.2087	43,000.4174	43,000.4194	2.0
9500.0047	19,000.0094	19,000.0082	−1.2	22,000.2246	44,000.4492	44,000.4488	−0.4
10,000.0188	20,000.0376	20,000.0317	−5.9	22,500.2542	45,000.5084	45,000.5080	−0.4
10,500.0234	21,000.0468	21,000.0385	−8.3	23,000.2712	46,000.5424	46,000.5407	−1.7
11,000.0233	22,000.0466	22,000.0453	−1.3	23,500.2810	47,000.5620	47,000.5594	−2.6
11,500.0170	23,000.0340	23,000.0335	−0.5	24,000.2927	48,000.5854	48,000.5836	−1.8
12,000.0209	24,000.0418	24,000.0403	−1.5	24,500.3135	49,000.6270	49,000.6259	−1.1
12,500.0137	25,000.0274	25,000.0282	0.8	25,000.3189	50,000.6378	50,000.6366	−1.2

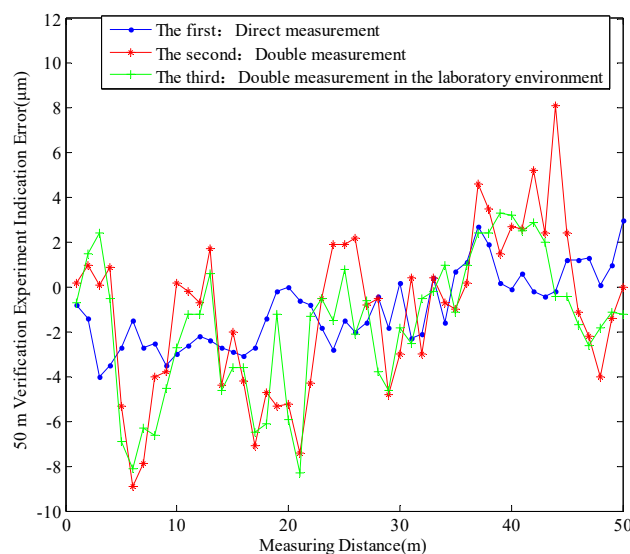


Figure 9. Comparison of indication errors from the 50-meter verification experiment.

4.4. Transverse Measurement Experiment

The aforementioned experiments demonstrate that the proposed double-range measurement method fulfills the requirements for the indication error of the laser tracker in the measurement of the identical direction. Furthermore, the obtained measurement results are highly satisfactory. To further investigate whether the laser tracker can achieve double-range transverse measurement, this study conducted the transverse measurement experiment in a controlled environment setting.

Figure 10 illustrates the transverse measurement. This figure is a representation of the measured drawing shown in Figure 7. The difference is that during the measurement, only one set of corner cube prisms was utilized, and the laser interferometer employed corresponds to the reflector A, which was in closest proximity to the corner cube prisms. The reflector employed in the laser tracker, as depicted in Figure 10, was securely affixed to the main body of the laser tracker. Table 9 shows the results of the transverse measurement based on Figure 10. The results indicate that the indication error in measurement fell within the millimeter range. The ratio between the measured value of the laser tracker and the nominal value of interferometer A exhibits a decrease as the measurement distance increases. Throughout the experiment, the laser tracker demonstrated significant oscillation and experienced light interruptions after the high-precision guide rail moved more than 550 mm. This suggests that the current method of using the laser tracker for transverse measurement does not meet the necessary requirements. Consequently, further investigation is necessary to develop a double-range measurement method. From this analysis, two conclusions can be derived as follows:

First, further optimization is required for the structure of the corner cube prism. The current design of the corner cube prism, with its cylindrical shape and inability to rotate around the Z-axis, limits the incident angle. To improve this, the corner cube prism should be redesigned with a spherical shape. Hence, further structural adjustments are necessary.

Second, the placement of the reflector used in the laser tracker requires optimization. Currently, there is a significant error due to the rotation of the laser tracker during measurements.

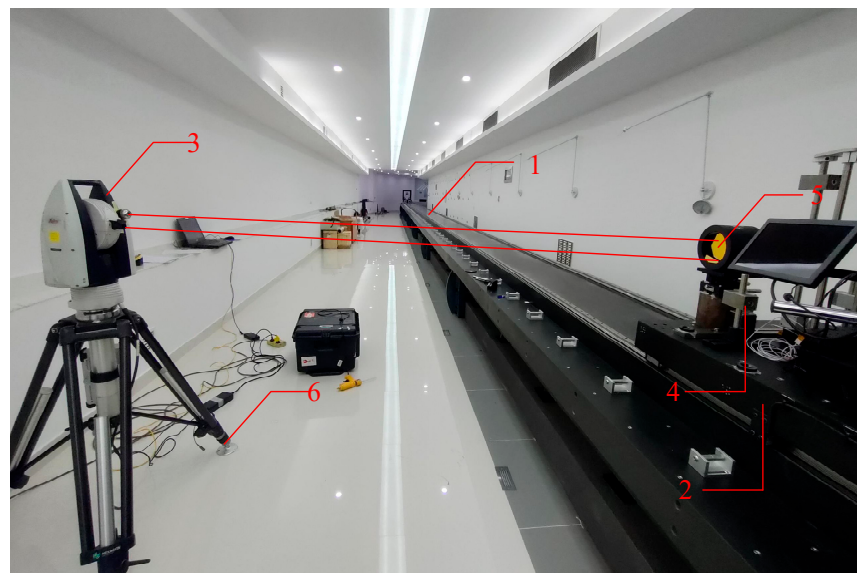


Figure 10. Transverse measurement. (1—guide rail, 2—second sliding platform, 3—tested laser tracker, 4—reflector A, 5—corner cube prism, 6—tripod with a fine adjustment mechanism).

Table 9. Results of the 1.1-m double-range measurement in a controlled environment setting (transverse measurement).

Interferometer A Measured Value (mm)	Interferometer A Nominal Value (mm)	Tracker Measured Value (mm)	Indication Error (mm)	Proportional Relationship
49.9976	99.9952	98.3266	1.7	0.9833
99.9936	199.9872	196.4885	3.5	0.9825
149.9962	299.9924	294.6218	5.4	0.9821
200.0003	400.0006	392.7322	7.3	0.9818
250.0025	500.0050	490.7917	9.2	0.9816
300.0030	600.0060	588.8210	11.2	0.9814
350.0032	700.0064	686.8230	13.2	0.9812
400.0042	800.0084	784.8147	15.2	0.9810
450.0011	900.0022	882.7623	17.2	0.9808
500.0031	1000.0062	980.7135	19.3	0.9807
549.9974	1099.9948	1078.5924	21.4	0.9805

5. Evaluation of Measurement Uncertainty for Indication Errors in the Identical-Directional Double-Range Measurement

5.1. Mathematical Model

The level of uncertainty associated with the vacuum wavelength of the laser interferometer is approximately 10^{-8} . The actual wavelength measured by the laser interferometer is determined by the environmental conditions, and the measurement uncertainty introduced by the corner cube prism can be disregarded. According to the Edlen equation, the displacement of the interferometer under a PTF environment is:

$$L_{PTF} = L + [93.0(T - 20) - 0.2683(P - 101325) + 0.0371(F - 1333)] \times 10^{-8} L \quad (1)$$

where L_{PTF} is the length measured by the laser interferometer under a controlled environment setting of 20 °C, in m; L is the length measured by the laser interferometer under a controlled environment setting, in m; T is the average air temperature along the optical path, in K; P is the air pressure along the optical path, in Pa; and F is the partial pressure exerted by water vapor in the air along the optical path, in Pa.

5.2. Analysis of Variances and Sensitivity Coefficients

The variables exhibit independence from one another. According to the propagation of uncertainty, this study demonstrates:

$$u_c^2(L_{PTF}) = u^2(L) + (93.0 \times 10^{-8} L)^2 u^2(T) + (0.2683 \times 10^{-8} L)^2 u^2(P) + (0.0371 \times 10^{-8} L)^2 u^2(F) + u^2(\delta L_1) + u^2(\delta L_2) \quad (2)$$

where δL_1 is the measurement error introduced by measurement repeatability, and δL_2 is the measurement error introduced by the reading error.

5.3. Analysis of Uncertainty Sources

5.3.1. Uncertainty Component u_1 (L) Introduced by Standard Instruments

From the calibration certificate of the laser interferometer system, it is evident that the uncertainty is $U = 0.1 \mu\text{m} + 1 \times 10^{-7}$ ($k = 2$). Assuming a normal distribution, the uncertainty component introduced by this source is:

$$u_1(L) \approx 5 \times 10^{-8} L \quad (3)$$

5.3.2. Standard Uncertainty $u(T)$, $u(P)$, $u(F)$ Introduced by Measurement Errors of Average Temperature T, Pressure P, and Vapor Pressure F in the Optical Path of Laser Interferometer

First, the standard uncertainty component introduced by environmental changes, specifically temperature, is denoted as $u(T)$. The measurement error of the average temperature of the optical path is 0.1 °C, and it is considered to have a uniform distribution:

$$u_2 = c_2 u(T) = 93.0 \times 10^{-8} \text{ L} \times 0.1 / \sqrt{3} = 5.4 \times 10^{-8} \text{ L} \quad (4)$$

Second, the standard uncertainty component introduced by environmental changes, specifically pressure, is denoted as $u(P)$. The measurement error of the pressure in the optical path is 11 Pa, and it is also considered to have a uniform distribution:

$$u_3 = c_3 u(P) = 0.2683 \times 10^{-8} \text{ L} \times 11 / \sqrt{3} = 1.7 \times 10^{-8} \text{ L} \quad (5)$$

Lastly, the standard uncertainty component introduced by environmental changes, specifically the partial pressure exerted by water vapor, is denoted as $u(F)$. The measurement error of the vapor pressure is 40 Pa, and it is treated as having a uniform distribution as well:

$$u_4 = c_4 u(F) = 0.0371 \times 10^{-8} \text{ L} \times 40 / \sqrt{3} = 0.9 \times 10^{-8} \text{ L} \quad (6)$$

5.3.3. Uncertainty Introduced by Reading Errors

First, the standard uncertainty was introduced by the resolution of the laser tracker. The tested laser tracker had a digital resolution of 1 μm and an interval half-width of 0.5 μm . Assuming a uniform distribution of $k = \sqrt{3}$, the uncertainty component introduced by the resolution is:

$$u_{5.1}(\Delta L_2) = 0.5 / 1.732 = 0.29 \mu\text{m} \quad (7)$$

Second, the measurement uncertainty is caused by reading drift. During the calibration process of the laser tracker, readings were simultaneously taken from both the tested laser tracker and the laser interferometer system. However, due to drift, there might be a maximum drift of 0.2 μm introduced by the time difference in readings. Assuming a uniform distribution, the measurement uncertainty caused by the drift is:

$$u_{5.2}(\Delta L_2) = 0.2 / 1.732 \approx 0.12 \mu\text{m} \quad (8)$$

5.3.4. Standard Uncertainty Introduced by Measurement Repeatability

The repeatability of measurements introduces a significant amount of uncertainty to the overall uncertainty. There are several factors that contribute to this measurement uncertainty, and it is likely to follow a normal distribution. To be cautious, this study selected a distribution with a smaller k value, such as a uniform distribution ($k = \sqrt{3}$). This study used the Bessel function to calculate the value at the position of 77 m. According to the standard deviation of 0.9 μm , the repeatability-induced uncertainty is calculated as:

$$u_6(\delta L_1) = 0.9 \mu\text{m} \quad (9)$$

This study also considered the larger value between resolution and repeatability as one of the components of uncertainty and found that the uncertainty introduced by measurement repeatability is relatively high.

5.4. Combined and Expanded Uncertainty

Table 10 shows the component of the measurement uncertainty of the indication error when the laser tracker is measured in the Identical-Directional Double-Range Measurement.

$$u_c^2(L) = u_1^2 + u_2^2 + u_3^2 + u_4^2 + u_{5.2}^2 + u_6^2 \quad (10)$$

$$U = 2u_c^2(L) \approx 1.0 \mu\text{m} + 0.2L \quad (k = 2) \quad L = (0 \sim 77 \text{ m}) \quad (11)$$

Within the entire range from 0 to 77 m, the expanded uncertainty of the indication error is $U = (1.0\sim 16.4) \mu\text{m}$ ($k = 2$).

Table 10. Standard uncertainty.

Standard Uncertainty Component	Source of Uncertainty	Value of Standard Uncertainty	k Value
u_1	Uncertainty of laser interferometer measurement	$5 \times 10^{-8} \text{ L}$	2
u_2	Error caused by temperature variation	$5.4 \times 10^{-8} \text{ L}$	$\sqrt{3}$
u_3	Error caused by pressure 1	$1.7 \times 10^{-8} \text{ L}$	$\sqrt{3}$
u_4	Error caused by pressure 2	$0.9 \times 10^{-8} \text{ L}$	$\sqrt{3}$
$u_{5,2}$	Error caused by reading drift	$0.12 \mu\text{m}$	$\sqrt{3}$
u_6	Standard uncertainty component caused by repeatability	$0.9 \mu\text{m}$	$\sqrt{3}$

6. Discussion

This paper focuses primarily on the static measurement of laser trackers. Upon conducting an extensive review of the existing literature, this study determines that the measurement of laser trackers in the identical direction has limitations when performing measurements across the full scale. To address this issue, the double-range measurement method was first used to study the indication error of the laser tracker by placing the hollow corner cube prism on a linear guide rail. The hollow corner cube prism mainly plays the role of retracing the optical path, and the linear guide rail is an important motion mechanism. The measurement data of the laser interferometer is used to quantify the collected measurement values. This method used in the experiment satisfies the requirements of the laser tracker, which offers a fresh idea and method that can be applied to investigate full-range measurements in other large-scale measuring instruments.

7. Conclusions

The analysis and research of indication errors under the static measurement of laser trackers are of utmost importance as they serve as a crucial instrument for geometric measurements. This study utilized the measurements of the laser interferometer system as nominal values and conducted an in-depth analysis of the measurement errors of the laser tracker. The comprehensive data analysis led to the derivation of five significant conclusions:

(1) When laser trackers are used for measurements of identical directions, the effects of triple-beam measurement, which eliminates the Abbe error, are significantly better than those achieved using a single-beam measurement, without eliminating the Abbe error. Both the triple-beam and single-beam measurements meet the measurement requirements of laser trackers. The error curves for both measurements are consistent in the triple-beam measurement as well as in the single-beam measurement. When the triple-beam laser was used for measurement, the maximum measurement repeatability was $7.1 \mu\text{m}$. When the single-beam laser was used for measurement, the maximum measurement repeatability was $11 \mu\text{m}$. Overall, both the triple-beam and single-beam measurements demonstrate good repeatability. Under a controlled experimental setting, when the triple-beam laser interferometer is used as the nominal value, the maximum indication error within a distance of 77 m for the laser tracker is $14.6 \mu\text{m}$. Similarly, when the single-beam laser interferometer is used as the nominal value, the maximum indication error within 77 m for the laser tracker is $-29.5 \mu\text{m}$;

(2) The laser tracker demonstrates exceptional single-point repeatability when measuring in an identical direction. In a controlled experimental setting, the laser tracker was subjected to two measurements at different positions. The results indicate that the

maximum single-point repeatability of the laser tracker is 0.5 μm at the 65 m position, 0.6 μm at the 70 m position, and 0.9 μm at the 77 m position;

(3) During the 50 m verification experiment in the identical direction, the laser tracker exhibited higher precision in the direct measurement as opposed to the double-range measurement. All three measurements met the required level of accuracy for the laser tracker, indirectly confirming the validity of the method used in the study. In a controlled experimental setting, the indication errors for the laser tracker were $-4.0 \mu\text{m}$ and $-8.9 \mu\text{m}$ for the direct measurement and double-range measurement, respectively. In a laboratory setting, the indication error for the laser tracker was $-8.3 \mu\text{m}$ for the double-range measurement;

(4) The measurement method used by the laser tracker does not meet the criteria for measuring transverse distances accurately. Therefore, further enhancements are necessary. The current double-range measurement indicates that the laser tracker has indication errors at the millimeter level, and the data are considerably beyond the expected range;

(5) When employing a laser tracker to conduct identical-directional measurements, the expanded uncertainty in the indication error is approximately $U \approx 1.0 \mu\text{m} + 0.2L$ ($k = 2$), where L varies between 0 and 77 m.

This paper mainly uses a large-scale high precision guide rail, laser interferometer and hollow corner cube prism as the measuring system and laser tracker as the measured object to comprehensively analyze the measurement indication errors of the laser tracker by setting up a complete set of measuring system. The proposed method is also suitable for the comparison measurement of other large-scale measuring instruments.

Author Contributions: Conceptualization, C.H. and L.X.; methodology, C.H.; software, C.H. and J.L.; validation, F.L., J.L. and X.Z.; data curation, C.H.; writing—original draft preparation, C.H.; writing—review and editing, Y.X.; visualization, C.H.; supervision, F.L.; project administration, L.X. All authors have read and agreed to the published version of the manuscript.

Funding: The research was funded by the National Key Research and Development Program of China (2021YFA1401100), the Innovation Group Project of Sichuan Province (20CXTD0090), and the National Natural Science Foundation of China (52202165).

Institutional Review Board Statement: Not applicable.

Informed Consent Statement: Not applicable.

Data Availability Statement: Data are contained within the article.

Conflicts of Interest: The authors declare no conflict of interest.

References

1. Sun, A.; Cao, T.; Wang, J.; Gan, X.; Gao, T. Technological Development Trends of Geometric Dimension Measurements of Large Parts in the High-end Equipment. *Metrol. Meas. Technol.* **2021**, *41*, 41–50.
2. Duan, T.; Fan, B.; Huang, H.; Xu, F.; Chen, Z.; Zou, F. Test method and experimental analysis of ATR accuracy in small-scale spherical coordinate measuring system. *Eng. Surv. Mapp.* **2023**, *32*, 80.
3. Ma, L. Research on Large-Scale Dimensional Calibration and Its Application in Measurement Transfer Chain. Ph.D. Thesis, Dalian University of Technology, Dalian, China, 2006.
4. Miao, D.; Li, J.; He, M.; Deng, X.; Li, L. Design and Development of 80 Meters Laser Interferometric Measurement Standard Device. *Ninth Int. Symp. Precis. Eng. Meas. Instrum.* **2015**, *9446*, 9446311–9446319. [[CrossRef](#)]
5. Wang, W.; Su, Y.; Ren, G. A Study on Dynamic Character of Laser Tracker. *Acta Metrol. Sin.* **2007**, *28*, 92.
6. Pan, T.; Fan, B.; Yi, W.; Xi, Q.; Yang, Z. Research on Evaluation Method of Laser Tracker Dynamic Accuracy. *Bull. Surv. Mapp.* **2016**, *5*, 54–56. [[CrossRef](#)]
7. Lv, F.; Hu, C.; Sun, H.; Li, W. Study on Dynamic Performance Parameters of Laser Tracker Based on Self-Developed Circular Trajectory Generator System. *Appl. Sci.* **2023**, *13*, 167. [[CrossRef](#)]
8. Morse, E.; Welty, V. Dynamic testing of laser trackers. *CIRP Ann.-Manuf. Technol.* **2015**, *64*, 475–478. [[CrossRef](#)]
9. Ma, Y.; Fan, B.; Huang, J. Research on the evaluation method of the accuracy of combined dynamic position and attitude measurement of multiple laser trackers. *Eng. Surv. Mapp.* **2021**, *30*, 55–59.
10. Xu, Y.; Zheng, Q.; Guan, X. Precision Analysis of Leica AT960 Absolute Laser Tracker. *J. Geomat.* **2020**, *45*, 8–12.
11. Liu, W.; Wang, Z.; Qu, X.; Ouyang, J. Error analysis of tracking mirror for laser tracker system. *Opt. Precis. Eng.* **2008**, *16*, 585–590.

12. Zhu, X.; Liu, L.; Chen, X. Measurement station optimization for laser tracker in-situ using based on Monte-Carlo simulation. *Comput. Integr. Manuf. Syst.* **2020**, *26*, 3001–3010.
13. Zhao, G.; Zhang, C.; Jing, X.; Sun, Z.; Zhang, Y.; Luo, M. Station-transfer measurement accuracy improvement of laser tracker based on photogrammetry. *Measurement* **2016**, *94*, 717–725. [[CrossRef](#)]
14. Acero, R.; Santolaria, J.; Pueo, M.; Brau, A. Verification of a laser tracker with an indexed metrology platform. *Int. J. Adv. Manuf. Technol.* **2016**, *84*, 595–606. [[CrossRef](#)]
15. Feng, T.; Cui, C.; Wang, S.; Dong, D.; Zhou, W. A study on the real-time compensation system based on Abbe principle for range accuracy of submicron measuring instrument. *Meas. Sci. Technol.* **2022**, *33*, 085019.
16. Conte, J.; Majarena, A.; Aguado, S.; Acero, R.; Santolaria, J. Calibration strategies of laser trackers based on network measurements. *Int. J. Adv. Manuf. Technol.* **2016**, *83*, 1161–1170. [[CrossRef](#)]
17. Mitchell, J.; Spence, A.; Hoang, M.; Free, A. Sensor fusion of laser trackers for use in large-scale precision metrology. *Int. Soc. Opt. Eng.* **2004**, *5263*, 57–65.
18. Cai, Q.; Zhao, M.; Liu, H.; Zheng, Y.; Zhang, H.; Song, L. Error Analysis Methodology for Indoor Baseline Field Based on Optical Path Folding. *Acta Metrol. Sin.* **2021**, *42*, 1142–1148.
19. Yang, Z.; Lei, Y. Calibrating laser rangefinder using fiber. *Opto-Electron. Eng.* **2007**, *34*, 139–144.
20. Shi, J.; He, Q.; Xu, Y. Research on Calibration of Laser Rangefinder Using Optical Fiber Baseline. *J. Nanjing Univ. Aeronaut. Astronaut.* **2012**, *44*, 830–834.
21. *GB/T 16857.10*; Geometrical Product Specifications (GPS)—Acceptance and Reverification Tests for Coordinate Measuring Systems (CMS)—Part 10: Laser Trackers. State Administration for Market Regulation: Beijing, China, 2022; pp. 1–45.

Disclaimer/Publisher’s Note: The statements, opinions and data contained in all publications are solely those of the individual author(s) and contributor(s) and not of MDPI and/or the editor(s). MDPI and/or the editor(s) disclaim responsibility for any injury to people or property resulting from any ideas, methods, instructions or products referred to in the content.